Schizophrenia Research 158 (2014) 204–212

Contents lists available at ScienceDirect

Schizophrenia Research

journal homepage: www.elsevier.com/locate/schres

The functional anatomy of schizophrenia: A dynamic causal modeling study of predictive coding

Noa Fogelson [a,*], Vladimir Litvak [b], Avi Peled [c,d], Miguel Fernandez-del-Olmo [e], Karl Friston [b,**]

[a] Joseph Sagol Neuroscience Center, Sheba Medical Center, Tel Hashomer, Israel
[b] The Wellcome Trust Centre for Neuroimaging, Institute of Neurology, UCL, London, UK
[c] Institute for Psychiatric Studies, Sha'ar Menashe Mental Health Center, Hadera, Israel
[d] B Rappaport Faculty of Medicine, Technion, Haifa, Israel
[e] Department of Physical Education, University of A Coruña, La Coruña, Spain

ARTICLE INFO

Article history:
Received 5 December 2013
Received in revised form 8 May 2014
Accepted 1 June 2014
Available online 3 July 2014

Keywords:
Dynamic causal modeling
Schizophrenia
EEG
Prediction
Connectivity

ABSTRACT

This paper tests the hypothesis that patients with schizophrenia have a deficit in selectively attending to predictable events. We used dynamic causal modeling (DCM) of electrophysiological responses – to predictable and unpredictable visual targets – to quantify the effective connectivity within and between cortical sources in the visual hierarchy in 25 schizophrenia patients and 25 age-matched controls. We found evidence for marked differences between normal subjects and schizophrenia patients in the strength of extrinsic backward connections from higher hierarchical levels to lower levels within the visual system. In addition, we show that not only do schizophrenia subjects have abnormal connectivity but also that they fail to adjust or optimize this connectivity when events can be predicted. Thus, the differential intrinsic recurrent connectivity observed during processing of predictable versus unpredictable targets was markedly attenuated in schizophrenia patients compared with controls, suggesting a failure to modulate the sensitivity of neurons responsible for passing sensory information of prediction errors up the visual cortical hierarchy. The findings support the proposed role of abnormal connectivity in the neuropathology and pathophysiology of schizophrenia.

1. Introduction

In a previous study we found consistent and large deficits in differential responses to predicted and unpredicted targets, using event related responses – as measured with EEG – in schizophrenia patients. In healthy adults predicted targets produced faster reaction times and shorter event-related potential (ERP) P3b latencies compared with targets after non-predictive sequences. Crucially, this context-dependent facilitation was attenuated in patients with schizophrenia (Fogelson et al., 2011).

In the current study, we revisit these differences in terms of the underlying functional and computational anatomy. We used the same data to estimate the effective connectivity or directed coupling within and among cortical sources — and differences in this coupling when stimuli are predictable. Connectivity was evaluated using dynamic causal modeling (DCM), where non-linear dynamic neuronal interactions between different regions are estimated (Friston et al., 2003). The particular hypothesis addressed by the current DCM study was that the excitability of superficial pyramidal cells differs between normal and schizophrenia subjects (i.e., excitability shows a main effect of group) and that predictability effects on this excitability would be attenuated in schizophrenia (i.e., excitability shows a group by condition interaction). Hierarchical Bayesian inference or predictive coding was used to test this hypothesis. In predictive coding top-down predictions (conditional expectations) are generated and compared with bottom-up sensory inputs to produce prediction errors. Prediction errors that are weighted in proportion to their expected precision are used to update higher level expectations, which in turn reduce lower-level prediction errors (Friston, 2008; Bastos et al., 2012). Thus, optimization of high-level predictions ensures an accurate prediction of sensory input.

Hierarchical Bayesian inference and predictive coding have been linked to schizophrenia and psychosis, so that precision corresponds to the confidence or certainty associated with a belief, and inappropriate beliefs about precision can lead to false inference (Adams et al., 2013).

* Correspondence to: N. Fogelson, The Joseph Sagol Neuroscience Center, Sheba Medical Center, Tel Hashomer, Ramat Gan 52621, Israel. Tel.: +972 35304753; fax: +972 35304752.
** Correspondence to: K. Friston, The Wellcome Trust Centre for Neuroimaging, Institute of Neurology, UCL, 12 Queen Square, London WC1N 3BG, UK. Fax: +44 207 813 1445.
E-mail addresses: nfogelson@gmail.com (N. Fogelson), k.friston@ucl.ac.uk (K. Friston).

http://dx.doi.org/10.1016/j.schres.2014.06.011

The suggestion is that psychotic symptoms can be explained in terms of a failure to represent precision regarding beliefs about the world (Adams et al., 2012, 2013), which corresponds to current thinking about the neuropathology of schizophrenia implicating the neuromodulation of postsynaptic excitability or cortical gain control; particularly in the supragranular cortical lamina (Harrison et al., 2011). This reflects the fact that many of the neurotransmitter receptors implicated in schizophrenia are expressed most densely in superficial layers (for example, dopamine — D1-R and NMDA-R) and are involved in the modulation of postsynaptic excitability or gain (Cohen and Servan-Schreiber, 1992; Friston and Frith, 1995; Friston, 1998; Wang, 2002; Coyle and Tsai, 2004; Stephan et al., 2006).

This is important from the point of view of predictive coding models of inference in the brain, because superficial pyramidal cells are thought to encode prediction error (Friston, 2008; Bastos et al., 2012). Superficial pyramidal cells convey prediction errors via extrinsic forward ascending connections (targeting spiny stellate cells), while deep pyramidal cells are thought to convey predictions, via extrinsic backward descending connections that target superficial pyramidal cells (Mumford, 1992; Friston, 2008; Bastos et al., 2012). In addition to the reciprocal exchange of signals through forward and backward extrinsic connectivity, the relative influence of prediction errors on higher-level expectations is itself optimized in terms of their relative weight and gain. This is thought to be implemented by intrinsic connectivity that controls the gain of neuronal populations broadcasting prediction errors (Friston, 2008; Bastos et al., 2012). The resulting excitability of superficial pyramidal cells corresponds (mathematically) to the precision of – or confidence in – the information conveyed by ascending prediction errors, that are weighted in proportion to their expected precision (Friston, 2008; Bastos et al., 2012). Precision is thought to be encoded by the post-synaptic gain of neurons that report prediction errors and has been used to explain both the psychophysical and electrophysiological correlates of attention, so that sensory processing channels that convey precise information are selectively enabled by an increase in their precision (Friston, 2008; Feldman and Friston, 2010; Bastos et al., 2012). Cortical bias or gain control is mediated by intrinsic inhibitory connections within cortical sources, which rescale prediction errors, in proportion to their precision, so that as precision increases intrinsic recurrent inhibition decreases (Abbott et al., 1997; Friston, 2008). Heuristically, precision can be thought of as a 'volume control' that is applied to prediction errors that are broadcast to revise predictions elsewhere in the hierarchy. In summary, optimization of high-level predictions reduces prediction error at lower levels, ensuring an accurate prediction of sensory input.

Currently, predictive coding schemes do not differentiate between the encoding associated with single cells and neuronal populations. In other words, predictions and prediction errors may be encoded by the firing rate averaged over populations of (superficial or deep pyramidal) cells. In our modeling, we assume that fluctuations in firing rates correspond to the ensemble averages implicit in neural mass models of cortical activity.

In neurobiological formulations of predictive coding (Mumford, 1992; Friston, 2005; Friston et al., 2005; Bastos et al., 2012), superficial pyramidal cells are thought to report precision-weighted prediction error: $\xi = \Pi(\mu_i - g(\mu_{i+1}))$, where μ_i corresponds to representations (posterior expectations) of states of the world at level i in a cortical hierarchy and $g(\mu_{i+1})$ corresponds to the top-down predictions of these expectations — based upon expectations in the level above. The precision of the ensuing prediction error – or mismatch – is modulated by the precision Π to weight the prediction errors in proportion to their expected salience. These prediction errors are then passed forward, to higher levels in the hierarchy, to adjust higher-level representations.

The encoding of precision – at any level of the cortical hierarchy – can be associated with the strength of inhibitory recurrent connections by noting that the expression for prediction errors is the solution to the following equation describing neuronal dynamics.

$$\xi = (\mu_i - g(\mu_{i+1})) - \Pi^{-1}\xi$$
$$\dot{\xi} = 0 \Rightarrow \xi = \Pi(\mu_i - g(\mu_{i+1}))$$

In this equation, Π^{-1} corresponds to the strength of recurrent inhibitory connections. This means that as precision increases, the strength of recurrent inhibitory connections decreases. We therefore use the strength of intrinsic inhibitory self-connections as a proxy for precision and how it changes with predictability.

In what follows, we focus on extrinsic (backward) connectivity – that conveys top-down predictions – and intrinsic (inhibitory recurrent) connectivity — that sets the effective gain and encodes precision. We hypothesized that there would be differences in both extrinsic and intrinsic connectivity in schizophrenia compared with age-matched controls (Dima et al., 2010; Adams et al., 2013; Fogelson et al., 2013). Furthermore, based on previous behavioral and ERP results (Fogelson et al., 2011), we predicted that there would be a significant effect of predictability in normal subjects that will be attenuated in schizophrenia. In other words, we conjectured that the underlying deficit in schizophrenia would be expressed as a failure to recognize sequential structure in successive stimuli and a consequent failure to attend to predictable sensory attributes. In predictive coding, this would correspond to a failure to increase the precision of precise sensory channels, which translates neurophysiology into a failure to modulate recurrent inhibitory connectivity. Heuristically, this means that schizophrenia patients find everything equally unpredictable, because they cannot selectively attend to predictable events through a failure of neuromodulatory gain control.

2. Materials and methods

2.1. Subjects

We used data from a subgroup of subjects reported in a previous study (Fogelson et al., 2011) consisting of 25 schizophrenia patients (mean age ± standard error of the mean = 33.1 ± 2.1 years, 3 females and 22 males) and 25 age-matched controls (mean age ± standard error of the mean = 33.7 ± 2.2 years, 3 females and 22 males). All the patients were hospitalized due to a recent psychotic episode. Patients were diagnosed with schizophrenia according to the Structured Clinical Interview for DMS-IV-TR and were rated for symptom severity using the Positive (SAPS) and Negative (SANS) Syndrome Scale (Andreasen and Olsen, 1982). Diagnostic categories of the patients included schizophrenia (mixture of disorganized and paranoid type, n = 14), paranoid type (n = 8), disorganized type (n = 2), and schizoaffective disorder (n = 1). Subjects with past history of neurologic disorders, drug or alcohol abuse were excluded. Patients received a daily mean dose chlorpromazine equivalent of 713 ± 109 mg (Table 1). No patient was sedated, or complained of sedation due to benzodiazepines at the day of the experiment. Mean illness duration was 10.6 ± 1.8 years. Mean SAPS and SANS scores were 69.8 ± 5.4 and 35.6 ± 6, respectively. All patients had normal or corrected-to-normal visual acuity. On the day of the experiment, the patients took their regular medications. Patients were matched by controls for age, sex and education. Age-matched controls had normal or corrected-to-normal visual acuity and had no history of psychiatric or neurological problems. The experimental procedures were approved by the local ethics committees. Written informed consent was obtained from all subjects participating in the study following a complete explanation of the study and procedures.

Table 1
Clinical details.

Patient	Disease duration (years)	SCID Diagnosis Schizophrenia	Age (years)	medication (daily dose, mg)	Antipsychotics (chlorpromazine equivalent)
1	1	Schizophrenia[a]	33	Clopenthixole 500	833
2	25	Paranoid	55	Haloperidole 200	333
3	6	Paranoid	23	Amisulpiride 400	400
4	25	Schizophrenia[a]	44	Clopenthixole 500	833
5	17	Schizophrenia[a]	23	Olanzepine 10	200
6	5	Schizophrenia[a]	38	Clopenthixole 30	1500
7	4	Schizophrenia[a]	35	Perphenazine 8	100
8	11	Schizophrenia[a]	28	Haloperidole 300	500
9	5	Schizophrenia[a]	33	Clopenthixole 500	833
10	15	Paranoid	50	Triflupromazine 100	2000
11	7	Schizophrenia[a]	28	Clopenthixole 30	1500
12	11	Schizoaffective	36	Clopenthixole 40	2000
13	6	Paranoid	29	Haloperidole 200	333
14	4	Schizophrenia[a]	26	Haloperidole 20	1000
15	2	Paranoid	19	Risperidone 4	200
16	4	Paranoid	23	Haloperidole 200	333
17	25	Paranoid	46	Clopenthixole 400	667
18	17	Paranoid	41	Haloperidole 20	1000
19	7	Disorganized	27	Olanzepine 20	400
20	7	Schizophrenia[a]	30	Haloperidole 20	1000
21	3	Schizophrenia[a]	27	Olanzepine 20	400
22	0.5	Schizophrenia	18	Olanzepine 20	400
23	30	Schizophrenia[a]	50	Risperidone 4	200
24	3	Disorganized	20	Risperidone 4	200
25	25	Schizophrenia[a]	46	Clopenthixole 400	667

[a] Patients diagnosed "schizophrenia" had mixtures of disorganized and paranoid DSM IV manifestations.

2.2. Procedure

Experimental procedures are described in Fogelson et al. (2011). Subjects sat 110 cm in-front of a 21-inch PC-computer screen. Stimuli were presented to either the left or right visual field 6° from a central fixation point. The subjects were asked to centrally fixate throughout the recording. Stimuli consisted of 15% targets (downward facing triangle) and 85% of equal amounts of three types of standards (triangles facing left, upwards and right, at 90 degree increments). In each block a total of 78 stimuli (12 targets, 22 of each standard type) were presented each for 150 ms with an inter-stimulus interval (ISI) of 1 s. Recording blocks consisted of targets preceded by either randomized sequences of standards or by sequences including a three-standard predictive sequence. The predictive sequence always consisted of the three standards of triangles facing left, up and right, always in that order. Each block consisted of 6 different randomized sequences of standards (3–8 standards long) preceding the target; and 6 sequences of standards (3–8 standards long) with a predictive sequence preceding the target in each (see Fig. 1). Each recording session comprised 14 different blocks, presented in randomized order. A single sequence of trials appeared on the right or left hemifield in a randomized order within each block. Blocks were counterbalanced such that there were equal numbers of stimuli presented to the right and left visual hemifields, across the blocks. The predictive sequence was always followed by a target. Subjects performed a brief training session to ensure that they were able to detect the target accurately. Subjects were then shown the predictive sequence and were told that it would be a 100% predictive of a target, but that targets would also appear randomly throughout the block. Subjects were asked to press a button each time a target was presented and to attend to the predictive sequence. Subjects then performed a brief training session to ensure that they were confident in the detection of the predictive sequence, as well as the targets, before the recording session began. Stimulus presentation was controlled using E-prime (Psychology Software Tools, Inc., Pittsburgh, USA).

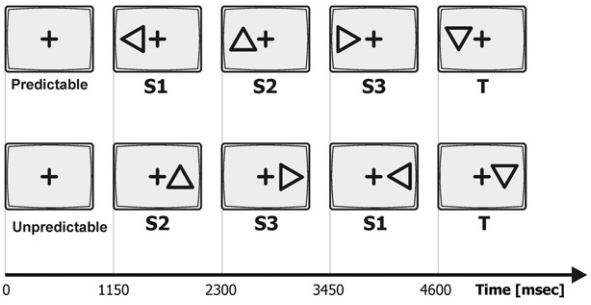

Fig. 1. Examples of a predictable (top) and unpredictable sequence (bottom) of the three standards S1, S2 and S3, preceded by the target (T). The predictive sequence is always S1 followed by S2 and then S3. Subjects respond to targets. Stimuli are presented to the left or right visual field. Inter-trial intervals, including duration of stimulus presentation (150 ms) are displayed.

2.3. Data acquisition

EEG was recorded from a 64 electrode array using the ActiveTwo system (Biosemi, The Netherlands). External electrodes above and below the right eye monitored vertical eye movements and electrodes placed laterally to the left and right eyes monitored horizontal eye movements. Signals were amplified and digitized at 512 Hz. All channels were re-referenced to averaged linked earlobes.

2.4. EEG preprocessing

Blink artifacts were detected using ICA (64 EEG electrodes were included), and the component identified as a blink was removed using the linear derivation function in Brain Vision Analyzer. Epochs containing misses (no button press 150–1150 ms post-stimulus onset) and eye saccades were excluded from further analysis. EEG epochs with amplitude of more than 75 μV at any electrode were excluded (performed using Brain Vision Analyzer version 1.05, Brain Products GmbH, Germany).

2.5. Behavioral analysis

Reaction times were calculated by averaging correct trials for predictable and unpredictable targets in each subject. Misses (no button press 150–1150 ms post-stimulus onset) were excluded from reaction

time analysis. Reaction times were analyzed using E-prime (Psychology Software Tools, Inc., Pittsburgh, USA). Analysis of variance (ANOVA) was performed with the Greenhouse–Geisser correction, followed by post-hoc parametric paired t-tests.

2.6. Dynamic causal modeling

We used standard DCM for ERP as implemented in SPM12 (Litvak et al., 2013). DCM for ERP uses a forward model based upon distributed sources that are coupled with extrinsic (between source) and intrinsic (within source) connections. Each source comprises several populations, each modeled with a pair of ordinary differential equations (according to the classic Jansen and Rit, 1995). The particular source model used here was the canonical microcircuit model (CMC, Bastos et al., 2012). This features four populations per source (spiny stellate cells, superficial pyramidal cells, inhibitory interneurons and deep pyramidal cells). The lamina specificity of forward and backward connections has been described elsewhere and – with the intrinsic connectivity – conforms to known anatomical and physiological constraints on neuronal circuitry (see Boly et al., 2011; Brown et al., 2011 for previous applications and a full description). In brief, forward connections arise from superficial pyramidal cells and target spiny stellate cells; whereas backward connections arise from deep pyramidal cells and target superficial pyramidal cells and inhibitory interneurons.

We were particularly interested in changes in backward and intrinsic (recurrent) connections. To this end, we use Bayesian model comparison (BMC) to ask whether the main effect of group was expressed in extrinsic forward connectivity, backward connectivity or both. To assess the group by condition interaction, we asked whether changes in intrinsic (recurrent) connectivity were evident in control subjects, schizophrenia subjects or both. To assess the evidence for each model, we used a series of dynamic causal models based upon the same underlying sources and connectivity architecture that was specified as follows.

2.7. Data feature and source specification

We elected to address our hypothesis using condition-specific grand average responses over all subjects within each group. This allowed us to directly test for the effect of group – and the effects of condition within each group – using Bayesian model comparison. Intuitively, this is like treating the grand averages as four different cells of a two-way factorial design with two factors (control versus schizophrenia and predictable versus unpredictable). To identify plausible sources we used a distributed source reconstruction (using all four grand averages) based on multiple sparse priors (with default settings as described in Litvak et al., 2011).

The grand average data were bandpass filtered between 2 and 32 Hz and windowed from 0 to 800 ms of peristimulus time. We used a canonical lead field based upon the standard MRI template and a boundary element model as implemented by default in SPM12 (Mattout et al., 2007). After source reconstruction, we then quantified the power of evoked responses (over all frequencies and peristimulus time) to produce the maximum intensity projection in Fig. 2. On the basis of this reconstruction, we identified seven sources corresponding (roughly) to maxima in the reconstruction (Fig. 2, right panel)., including V1, right and left V5, right and left inferotemporal sources (IT) and bilateral superior parietal sources (PC).

Exogenous (stimulus related) input was modeled as Gaussian functions centered at 180 and 240 ms (with a standard deviation of 16 and 32 ms). These two input components were delivered to V1 (via the lateral geniculate) and PC to model extra-geniculate input or later (recognition-related) inputs from unmodeled sources. The ensuing models were optimized to explain that the observed ERP is at the scalp level by adjusting their connectivity parameters in the usual way — this is known as model inversion or fitting. The products of this inversion are posterior estimates of the coupling strength and the evidence or marginal likelihood for each model. For all DCM inversions, we used data from 100 to 600 ms of peristimulus time (to cover visually evoked responses). To de-noise the data and improve computational efficacy,

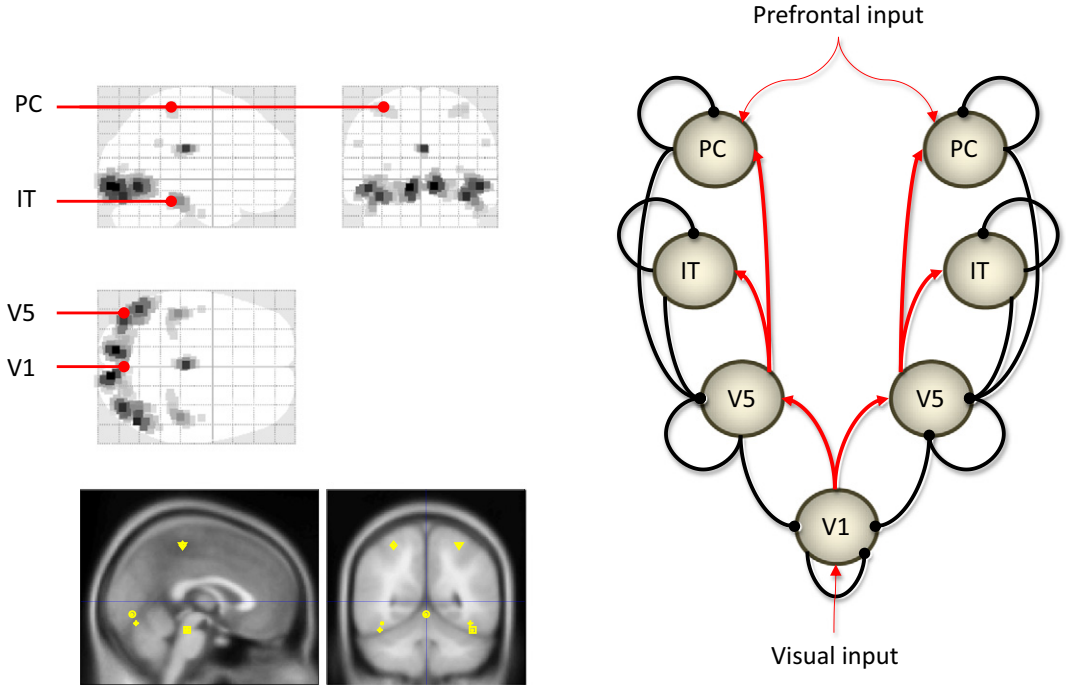

Fig. 2. Source locations modeled as small cortical patches (left panel) include: a midline visual source (V1), right and left sources near the temporoparietal junction (V5), right and left inferotemporal sources (IT) and bilateral superior parietal sources (PC). The distributed network connecting these sources (right panel) include top-down connections from PC and IT to V5 that then send backward connections to V1 (black lines); reciprocal forward connections (red lines); and intrinsic connections for each source (black loops).

we fitted the first eight principal components or modes of the scalp data. Finally, our sources were modeled as small cortical patches – centered on the source locations in Fig. 2 – as described previously (Daunizeau et al., 2006). The vertices of these localized sources used the same lead fields as in the source reconstruction above.

2.8. Model space and Bayesian model comparison

We estimated a full model in which all extrinsic (forwards and backwards) and intrinsic connections could differ in a generic way between the normal and schizophrenic responses. However, since our hypothesis centered on the backwards and intrinsic connections that target superficial pyramidal cells (Friston, 2008; Bastos et al., 2012), we restricted differences between predictable and unpredictable conditions to intrinsic connections that are thought to mediate gain control. This enabled us to ask whether there were any differences between normal and schizophrenia subjects (averaged over conditions) and whether condition specific differences in the intrinsic connectivity of both groups was necessary to explain observed responses. To answer these questions we used Bayesian model comparison based upon (a variational free energy) approximation to log evidence provided by model inversion (Friston and Penny, 2011).

Having identified the model with the greatest evidence – for the main effects of group and the simple main effects of condition – we then examined the posterior estimates of the effective connectivity under this model (Friston and Penny, 2011). This allowed us to characterize the effects quantitatively and to interpret them in computational (predictive coding) terms and in relation to the pathophysiology of schizophrenia.

3. Results

3.1. Behavioral results

To compare the reaction times (RT) for the targets between schizophrenia patients (SZ) and controls, we performed an ANOVA with group (SZ patients, controls) as the between-subject factor and condition (predictable, unpredictable targets) as the repeated measures factor. There was a main effect for condition ($F(1,60) = 147.36$, $p < .0001$) and a significant condition x group interaction ($F(1,60) = 87.75$, $p < .0001$). Post hoc t-tests showed that in controls RTs for predictable targets (mean RT = 298 ± 17 ms) were shorter than those for unpredictable targets (mean RT = 442 ± 13 ms, $t(29) = 10.8$, $p < .0001$). In the SZ patients, RTs for predictable targets (mean RT = 449 ± 14 ms) were also shorter than unpredictable targets (mean RT = 467 ± 14 ms, $t(31) = 5.39$, $p < .0001$). However, independent t-tests revealed that the difference in RT between target conditions was significantly larger in controls (mean RT difference = 144 ± 13 ms) compared to SZ patients (mean RT difference = 19 ± 4 ms, $t(60) = 9.37$, $p < .0001$). In addition, RTs for predictable targets were shorter in controls compared to patients ($t(60) = 6.97$, $p < .0001$), while RTs for unpredictable targets were not significantly different between patients and controls ($t(60) = 1.33$, $p = 0.19$).

3.2. Models and sources

We identified seven sources corresponding (roughly) to maxima in the source reconstruction of electroencephalographic (ERP) responses to visual targets, following predictive and nonpredictive sequences (Fig. 2, left panel). These sources included a midline visual source (V1), right and left sources near the temporoparietal junction (V5), right and left inferotemporal sources (IT) and bilateral superior parietal sources (PC). The temporal and parietal sources sent top-down connections to the extrastriate (V5) sources that then sent backward connections to the V1 source. These backward connections were reciprocated by extrinsic forward connections to produce a simple visual hierarchy. This distributed network or hierarchy is shown in Fig. 2 (right panel).

Fig. 3 shows that the coupling estimates were able to reproduce the observed ERP responses. The left panels show butterfly plots comparing the predicted and observed ERPs over all channels, for each of the four grand average responses (predictable and unpredictable in normal and schizophrenia subjects). The same data and predictions are shown in the right panels, in terms of the spatial modes used during model inversion. The first and third modes reveal the differences between predictable and unpredictable conditions. One can see a pronounced difference in normal subjects (compare red and blue traces) that is expressed both in terms of a greater latency and amplitude of response components around 300 to 400 ms. Crucially this difference is markedly attenuated in the responses of schizophrenia patients (green and magenta).

The model used to produce these predictions, involved group and condition specific changes in extrinsic and intrinsic connections. This full model gave the best explanation for the effect of group (normal versus schizophrenia), condition (predictable versus unpredictable) and their interaction. This is important because it suggests that in addition to a main effect of schizophrenia on the ERPs, there was a differential effect of predictability between control and schizophrenia subjects.

3.3. Schizophrenia vs. controls

Fig. 4 (left panel) shows the results of Bayesian model comparison (BMC), testing for differences in extrinsic connections between control and schizophrenia subjects (relative to a null model with just differences in intrinsic connectivity). It can be seen that the model with both forward and backward differences has substantially more evidence, with a log Bayes factor (log evidence difference) of over ten. A difference in log evidence of three is generally taken to be significant because this suggests an odds ratio of about one in 20, or one in exp(3). The second best model allows for differences in backward connections but not forward connectivity. This model ranking is consistent with the posterior estimates of neuronal coupling shown in Fig. 5 (upper left panel). These estimates are shown in image format as a connectivity matrix of posterior expectations (or maximum a posteriori – MAP – estimates). The model selection suggests that connectivity in schizophrenia patients is greater than normal subjects, and that these differences are more marked in the backward, relative to the forward, connections. In fact, the middle panel (showing MAP estimates of free extrinsic connection parameters and their 90% posterior confidence intervals) shows that nearly every connection is greater in schizophrenia and that the greatest differences are in the backward connections from (right) inferotemporal sources (IT) to the temporoparietal junction (V5) and from V5 to the early visual source (V1).

3.4. Effects of predictability in control subjects

Fig. 4 shows the BMC results for the effects of condition (predicted vs. unpredictable) in terms of models that allowed for changes in intrinsic connectivity. Here, the model with changes in recurrent self-inhibition of superficial pyramidal cells in both control and schizophrenia subjects supervenes (again, with a log Bayes factor of over ten). Interestingly, the (second best) model that includes difference in, and only in, controls has much more evidence than the converse model that allows for changes in, and only in, schizophrenia patients. This suggests that although there are condition-dependent changes in intrinsic connectivity in both groups, these changes are more evident in normal subjects.

Again, this is consistent with the quantitative MAP estimates of coupling in Fig. 5: Here, we show that normal subjects decrease recurrent inhibition at the highest parietal level of the hierarchy, when outcomes were predicted. This context-dependent effect is accompanied by a decrease in self-inhibition in visual (V1 and V5) sources and a

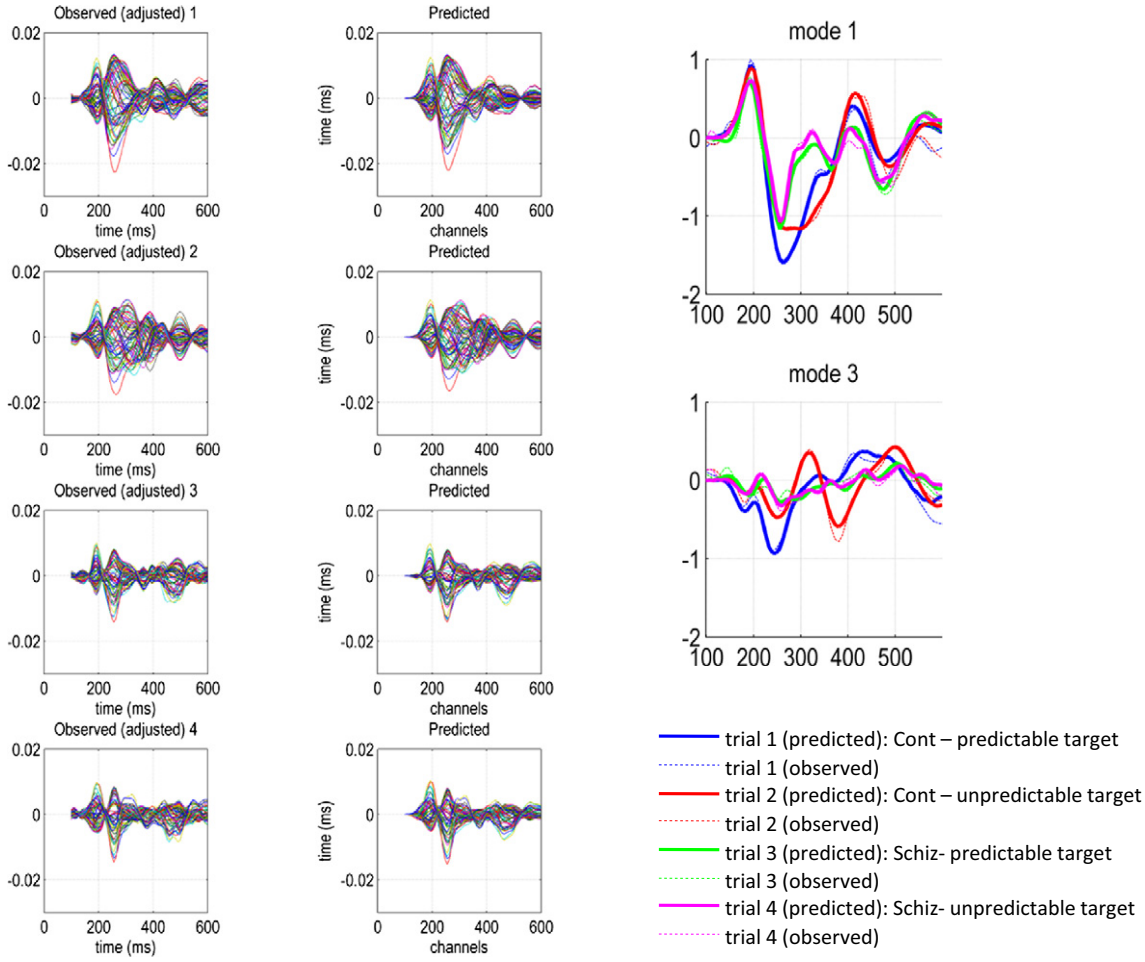

Fig. 3. Plots comparing the predicted and observed ERPs over all channels, for each of the four grand average responses (left panel) including: Controls-predictable targets (1), Controls-unpredictable targets (2), Schizophrenia-predictable targets (3), and Schizophrenia-unpredictable targets (4). Principal spatial modes 1 and 3 (left panel) show a pronounced difference in the evoked responses of normal subjects to predictable and unpredictable targets (compare red and blue traces) around 300 to 400 ms, while this difference is markedly attenuated in the schizophrenia patients (green and magenta).

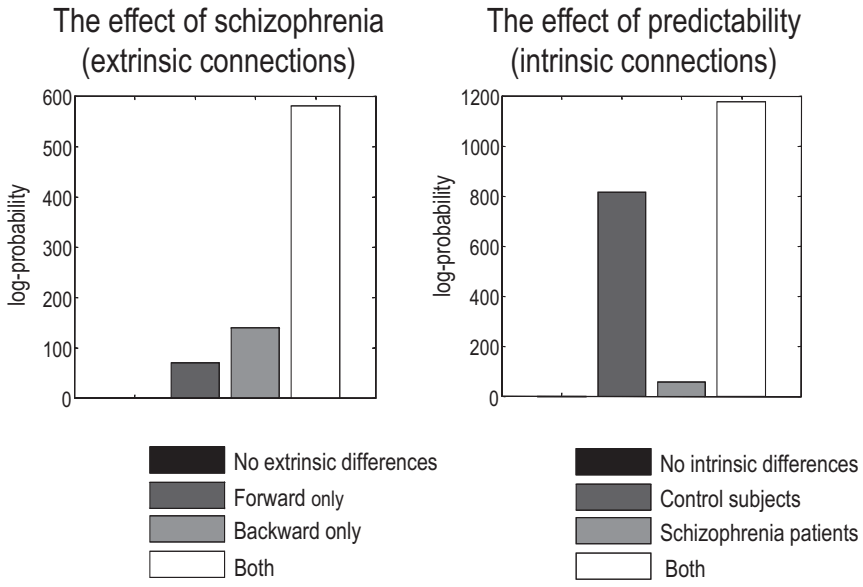

Fig. 4. Bayesian model comparison (BMC) testing for differences in extrinsic connections between controls and schizophrenia patients (left panel) and for changes in intrinsic connectivity between predictable and unpredictable target conditions (right panel). The model with both forward and backward differences shows the greatest evidence.

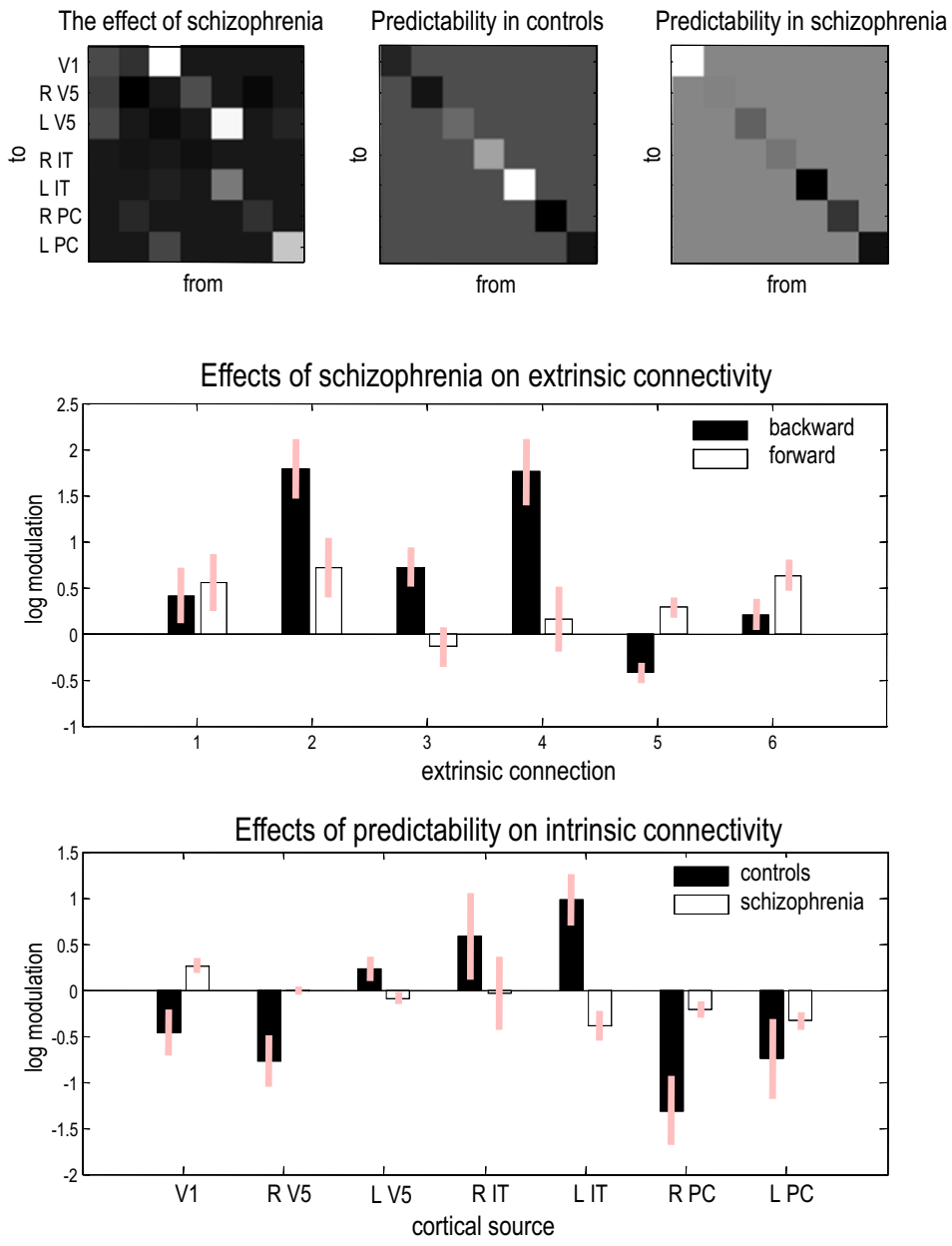

Fig. 5. Upper panel displays matrices of posterior expectations (MAP estimates) of changes in connectivity among the midline visual source (V1), right (R) and left (L) sources near the temporoparietal junction (RV5, LV5), inferotemporal sources (RIT, LIT) and superior parietal sources (RPC, LPC). Changes in schizophrenia vs. controls (left panel) are in both extrinsic and intrinsic connections, while changes due to predictability in control subjects (right panel) and schizophrenia patients (left panel) are limited to intrinsic connections (the gray scale is arbitrary — see lower panels for quantitative results). Middle panel displays MAP estimates of free (log scaling of) extrinsic connection parameters and their 90% posterior confidence intervals, for schizophrenia patients compared with controls, for backward and forward connections. The 6 extrinsic connections are between: 1 — V1 and LV5, 2 — V1 and RV5, 3 — LV5 and LIT, 4 — RV5 and RIT, 5 — LIT and LPC, and 6 — RIT and RPC. Lower panel displays MAP estimates of (log scaling of) intrinsic connection parameters and their 90% posterior confidence intervals, for predictable versus unpredictable targets, across patients and controls.

complementary increase in inferotemporal sources. However, these context-sensitive modulatory responses were seen only in controls.

3.5. Effects of predictability in schizophrenia patients

Fig. 5 (lower panel) shows that the changes in self-inhibition associated with predicted stimuli are markedly attenuated in the schizophrenic responses. In every source, the magnitude of the modulatory response is nearly an order of magnitude less than in normal subjects. Furthermore, there is even a suggestion of a reversal of the bias toward bottom-up processing of predicted stimuli — with a slight increase in self inhibition (decrease in precision) in V1.

4. Discussion

The main findings of the study are two-fold. First, we show that the backward connectivity in schizophrenia patients is greater than normal subjects during target detection, with greatest differences in the backward connections from (right) inferotemporal sources (IT) to the temporoparietal junction (V5) and from V5 to the early visual source (V1). These coupling differences suggest an increased sensitivity of the neuronal targets (superficial pyramidal cell populations and inhibitory interneurons), speaking to an abnormal gain control of neurons in superficial layers. These findings support the proposed role of abnormal modulation of synaptic efficacy in the pathophysiology of schizophrenia (Friston and Frith, 1995; Friston, 1998; Stephan et al., 2006). Our

findings are also in line with other studies showing abnormal top-down connectivity in schizophrenia during the performance of cognitive tasks (Dima et al., 2010; Fogelson et al., 2013).

Second, we show that not only do schizophrenia subjects have abnormal connectivity but that they fail to adjust or optimize this connectivity when events can be predicted. Thus, context-dependent effects on recurrent inhibition observed in normal subjects are attenuated in schizophrenia patients. These findings are supported by behavioral and ERP results, replicating earlier findings (Fogelson et al., 2011), showing an attenuation of the differences in RT and P3b latency between predictive and unpredictable targets, as well as a specific prolongation of these measures for predicted (but not for unpredictable) targets in schizophrenia patients compared with controls. In normal subjects, during processing of predicted targets, recurrent self inhibition decreases at the highest parietal level of the hierarchy (PC) and in visual (V1 and V5) sources, compared with unpredictable targets. This decrease is accompanied by a complementary increase in inferotemporal sources. The parietal lobes are involved in voluntary selection of attention (Posner et al., 1984; Corbetta et al., 2000), while inferotemporal cortex is associated with high-level stimulus categorization and task-relevant visual representation (Schendan and Stern, 2008; Woloszyn and Sheinberg, 2009). Thus, the observed effects suggest an adaptive increase in the precision of – or confidence in – high-level expectations that provide top-down predictions. These effects are consistent with an attentional selection of visual processing pathways that assigns greater precision to (predictable) visual input and renders high-level categorization (in the inferotemporal sources) more sensitive to bottom up sensory influences. In terms of predictive coding, this enables bottom-up prediction errors to inform high-level expectations more efficiently. Prediction errors throughout the hierarchy are then resolved more quickly — providing a computational explanation for the reduced latency of late (endogenous) evoked responses when visual input is predicted. Crucially, these context-sensitive modulatory responses were markedly attenuated in the schizophrenia patients, across parietal, inferotemporal and visual cortical sources, suggesting a failure of modulation of recurrent inhibitory connections. This is in line with theories implicating GABAergic neurotransmission in the neuromodulatory abnormalities of schizophrenia (Benes and Berretta, 2001; Wassef et al., 2003; Coyle, 2004; Lewis et al., 2004), such as impaired activation of GABAergic interneurons (Adams et al., 2013). Notice here, that the effective connectivity subsumes polysynaptic coupling and – in particular – recurrent inhibitory connections among (excitatory) pyramidal cells involve polysynaptic connections through inhibitory interneurons, which play a key role in canonical microcircuit models of predictive coding (Bastos et al., 2012). Computationally – in terms of predictive coding – this fits with abnormalities in attributing an appropriate degree of confidence or precision to various levels of representations in hierarchical (Bayesian) perceptual inference (Corlett et al., 2011; Adams et al., 2012, 2013). Thus, the abnormal modulation that was observed in the schizophrenia patients during processing of predicted targets may be explained in terms of abnormalities in the precision or confidence ascribed to predictions and sensory input at various cortical levels of the visual hierarchy. These findings give further support to the proposition that schizophrenia is a disorder of functional connectivity (Friston and Frith, 1995) and precision encoding (Adams et al., 2013).

In conclusion, we have used a biophysically informed model of visually evoked responses in normal and schizophrenia subjects to quantify the differences in coupling within and between cortical sources. We found evidence for marked differences between normal and schizophrenia subjects that were expressed predominantly in backwards connections from higher hierarchical levels to lower levels. However, our key finding was that schizophrenia patients had a markedly attenuated differential response to stimuli that could and could not be predicted on the basis of preceding stimuli. Dynamic causal modeling of these responses suggest that these attenuated differences (c.f., classical P3b updating differences) can be explained in terms of a failure to adjust or modulate the sensitivity of neurons responsible for passing sensory information (prediction errors) up the visual cortical hierarchy. In other words, normal subjects appear to exploit the predictability inherent in the sequence to endow predicted visual input (early visual prediction errors) with greater precision, leading to a more efficient resolution of uncertainty about the causes of that input. However –according to our results – schizophrenia subjects fail to exploit predictability in this context-dependent fashion and process predictable and unpredictable stimuli as if they were the same. This is consistent with an abnormality of neuromodulation, or its top-down control, that might underlie false inference — and is consistent with the neuropathology and pathophysiology of schizophrenia.

Funding

This work was supported by the Wellcome Trust and the Spanish Ministry of Science and Innovation [PSI2012-34212, DEP2011-22466].

Contributors

N.F. designed the study, recorded data, wrote the manuscript and contributed to the analysis of data. V.L. contributed to analysis of data and the writing of the manuscript. A.P. recruited patients and provided clinical data. M.F. recruited control subjects and recorded data. K.F. conceived analysis design and conceptual framework, analyzed data and wrote the manuscript.

Conflict of interest

All authors declare no conflict of interest.

Acknowledgments

The authors would like to thank the patients for participating in the study.

References

Abbott, L.F., Varela, J.A., Sen, K., Nelson, S.B., 1997. Synaptic depression and cortical gain control. Science 275, 220–224.
Adams, R.A., Perrinet, L.U., Friston, K., 2012. Smooth pursuit and visual occlusion: active inference and oculomotor control in schizophrenia. PLoS ONE 7, e47502.
Adams, R.A., Stephan, K.E., Brown, H.R., Frith, C.D., Friston, K.J., 2013. The computational anatomy of psychosis. Front. Psychiatry 4, 47.
Andreasen, N.C., Olsen, S., 1982. Negative and positive Schizophrenia: definition and validation. Arch. Gen. Psychiatry 39, 789–794.
Bastos, A.M., Usrey, W.M., Adams, R.A., Mangun, G.R., Fries, P., Friston, K.J., 2012. Canonical microcircuits for predictive coding. Neuron 76, 695–711.
Benes, F.M., Berretta, S., 2001. GABAergic interneurons: implications for understanding schizophrenia and bipolar disorder. Neuropsychopharmacology 25, 1–27.
Boly, M., Garrido, M.I., Gosseries, O., Bruno, M.A., Boveroux, P., Schnakers, C., Massimini, M., Litvak, V., Laureys, S., Friston, K., 2011. Preserved feedforward but impaired top-down processes in the vegetative state. Science 332, 858–862.
Brown, H., Friston, K., Bestmann, S., 2011. Active inference, attention, and motor preparation. Front. Psychol. 2, 218.
Cohen, J.D., Servan-Schreiber, D., 1992. Context, cortex, and dopamine: a connectionist approach to behavior and biology in schizophrenia. Psychol. Rev. 99, 45–77.
Corbetta, M., Kincade, J.M., Ollinger, J.M., McAvoy, M.P., Shulman, G.L., 2000. Voluntary orienting is dissociated from target detection in human posterior parietal cortex. Nat. Neurosci. 3, 292–297.
Corlett, P.R., Honey, G.D., Krystal, J.H., Fletcher, P.C., 2011. Glutamatergic model psychoses: prediction error, learning, and inference. Neuropsychopharmacology 36, 294–315.
Coyle, J.T., 2004. The GABA-glutamate connection in schizophrenia: which is the proximate cause? Biochem. Pharmacol. 68, 1507–1514.
Coyle, J.T., Tsai, G., 2004. NMDA receptor function, neuroplasticity, and the pathophysiology of schizophrenia. Int. Rev. Neurobiol. 59, 491–515.
Daunizeau, J., Mattout, J., Clonda, D., Goulard, B., Benali, H., Lina, J.M., 2006. Bayesian spatio-temporal approach for EEG source reconstruction: conciliating ECD and distributed models. IEEE Trans. Biomed. Eng. 53, 503–516.
Dima, D., Dietrich, D.E., Dillo, W., Emrich, H.M., 2010. Impaired top-down processes in schizophrenia: a DCM study of ERPs. NeuroImage 52, 824–832.
Feldman, H., Friston, K.J., 2010. Attention, uncertainty, and free-energy. Front. Hum. Neurosci. 4, 215.
Fogelson, N., Ribolsi, M., Fernandez-del-Olmo, M., Rubino, I.A., Romeo, D., Koch, G., Peled, A., 2011. Neural correlates of local contextual processing deficits in schizophrenic patients. Psychophysiology 48, 1217–1226.
Fogelson, N., Li, L., Li, Y., Fernandez-del-Olmo, M., Santos-Garcia, D., Peled, A., 2013. Functional connectivity during contextual processing in schizophrenia and Parkinson's disease. Brain Cogn. 82, 243–253.
Friston, K.J., 1998. The disconnection hypothesis. Schizophr. Res. 30, 115–125.
Friston, K.J., 2005. A theory of cortical responses. Philos. Trans. R. Soc. B 360, 815–883.
Friston, K., 2008. Hierarchical models in the brain. PLoS Comput. Biol. 4, e1000211.
Friston, K.J., Frith, C.D., 1995. Schizophrenia: a disconnection syndrome? Clin. Neurosci. 3, 89–97.

Friston, K., Penny, W., 2011. Post hoc Bayesian model selection. NeuroImage 56, 2089–2099.
Friston, K.J., Harrison, L., Penny, W., 2003. Dynamic causal modelling. NeuroImage 19, 1273–1302.
Friston, K.J., Penny, W., David, O., 2005. Modeling brain responses. Int. Rev. Neurobiol. 66, 89–124.
Harrison, P.J., Lewis, D.A., Kleinman, J.E., 2011. Neuropathology of schizophrenia. In: Weinbergerand, D.R., Harrison, P.J. (Eds.), Schizophrenia. Wiley-Blackwell, Oxford, pp. 372–392.
Jansen, B.H., Rit, V.G., 1995. Electroencephalogram and visual evoked potential generation in a mathematical model of coupled cortical columns. Biol. Cybern. 73, 357–366.
Lewis, D.A., Volk, D.W., Hashimoto, T., 2004. Selective alterations in prefrontal cortical GABA neurotransmission in schizophrenia: a novel target for the treatment of working memory dysfunction. Psychopharmacology 174, 143–150.
Litvak, V., Mattout, J., Kiebel, S., Phillips, C., Henson, R., Kilner, J., Barnes, G., Oostenveld, R., Daunizeau, J., Flandin, G., Penny, W., Friston, K., 2011. EEG and MEG data analysis in SPM8. Comput. Intell. Neurosci. 2011, 852961.
Litvak, V., Jha, A., Flandin, G., Friston, K., 2013. Convolution models for induced electromagnetic responses. NeuroImage 64, 388–398.
Mattout, J., Henson, R.N., Friston, K.J., 2007. Canonical source reconstruction for MEG. Comput. Intell. Neurosci. 2007, 67613.
Mumford, D., 1992. On the computational architecture of the neocortex. II. The role of cortico-cortical loops. Biol. Cybern. 66, 241–251.
Posner, M.I., Walker, J.A., Friedrich, F.J., Rafal, R.D., 1984. Effects of parietal injury on covert orienting of attention. J. Neurosci. 4, 1863–1874.
Schendan, H.E., Stern, C.E., 2008. Where vision meets memory: prefrontal-posterior networks for visual object constancy during categorization and recognition. Cereb. Cortex 18, 1695–1711.
Stephan, K.E., Baldeweg, T., Friston, K.J., 2006. Synaptic plasticity and dysconnection in schizophrenia. Biol. Psychiatry 59, 929–939.
Wang, X.-J., 2002. Probabilistic decision making by slow reverberation in cortical circuits. Neuron 36, 955–968.
Wassef, A., Baker, J., Kochan, L.D., 2003. GABA and schizophrenia: a review of basic science and clinical studies. J. Clin. Psychopharmacol. 23, 601–640.
Woloszyn, L., Sheinberg, D.L., 2009. Neural dynamics in inferior temporal cortex during a visual working memory task. J. Neurosci. 29, 5494–5507.